MRS Symposium Proceedings, Ferroelectric Thin Films III, 1993.

PHOTO-INDUCED AND ELECTROOPTIC PROPERTIES OF (Pb,La)(Zr,Ti)O_3 FILMS

D. DIMOS, W.L. WARREN, and B.A. TUTTLE
Sandia National Laboratories, Albuquerque, NM 87185

ABSTRACT

Photo-induced changes in the hysteresis behavior of sol-gel derived Pb(Zr,Ti)O_3 (PZT) and (Pb,La)(Zr,Ti)O_3 (PLZT) films have been characterized. The film photosensitivity has been evaluated with respect to the magnitude of the effects, the time response and the spectral dependence. Photo-induced hysteresis changes exhibit a stretched-exponential time dependence, which implies a dispersive mechanism. The spectral dependence is strongly peaked at the band edge (~3.4 eV), which indicates that generation of electron-hole pairs in the material is critical. The photo-induced hysteresis changes are reproducible and stable, which indicates that the controlling charge traps are stable. However, improvements in film photosensitivity will be required to develop these materials for optical memory applications.

INTRODUCTION

There is an increasing demand today for devices capable of storing and processing large quantities of optical information, including random-access optical memories, image comparators, and spatial light modulators (SLMs). Ferroelectric thin films, especially those based on PLZT solid solutions, exhibit photoferroelectric and electrooptic responses that make them good candidate materials for many optical-information storage, display and processing applications [1-5]. To store optically-generated information, light is used, in possible combination with an applied bias, to locally change the polarization state of the film. For optical readout, the polarization-dependent birefringence can be used to modulate the reflected (or transmitted) light intensity.

There have been many studies of electrooptic responses in PZT and PLZT films, which show that thin-film electrooptic properties are comparable to PLZT ceramics of similar compositions. Furthermore, the size of the electrooptic effects in films should be sufficient for optical readout with good signal-to-noise, especially if enhanced by using suitable etalon techniques [6]. In addition, photo-induced effects for optical storage have been extensively studied in PLZT ceramics [7-10]; however, relatively little has been reported about comparable effects in ferroelectric films [11-12]. Consequently, photo-induced responses in PZT and PLZT films have been studied with an emphasis on optical-information storage applications.

In this paper, photo-induced changes in the hysteresis behavior of sol-gel derived PZT and PLZT films are reported for various compositions, substrate types, and electrode materials. The various types of photo-induced effects and their magnitudes are discussed. An initial evaluation of the photosensitivity with respect to the time response and the spectral dependence is also presented. Since the photo-induced responses are intimately related to charge trapping, electron paramagnetic resonance (EPR) has been used to examine photo-induced charge traps. All of these studies provide important information about the photoferroelectric mechanisms in PLZT films and give a starting point for considering device performance.

EXPERIMENTAL

PZT and PLZT films were fabricated by spin coating using a metal alkoxide solution; the precursors were lead (IV) acetate, lanthanum acetate, zirconium butoxide butanol, and titanium isoproxide. A comprehensive description of the procedure has been previously published [13,14]. The desired film thickness was achieved by depositing multiple layers. After each layer was deposited, a 300°C bake was used to drive off volatile organics. Both oxidized silicon wafers and MgO single crystals were used as substrates. The base electrode was either Pt or RuO_x ($x \leq 2$), which gave four different substrate types: $Pt/Ti/SiO_2/Si$, $RuO_x/Ti/SiO_2/Si$, Pt/MgO, and $RuO_x/Ti/MgO$; the Ti layer was to promote adhesion. For the Pt/MgO samples, the Pt was deposited at approximately 600°C to achieve a high degree of [100] orientation. The films on Si subtrates were fired at 650°C for about 30 min. The films on MgO substrates were processed using rapid thermal annealing to 650°C; a highly-oriented [001] PZT film was obtained with the oriented Pt electrode. Both procedures yielded films that were essentially single-phase perovskite and had columnar microstructures with a lateral grain size of 100-150 nm. Films in excess of 500 nm thick were prepared by firing after every 4 layers to avoid cracking during densification.

Top electrodes (1-3 mm diameter) were sputter deposited to establish a parallel-plate capacitor geometry. To allow investigation of photo-induced effects, optically-transparent indium tin oxide (ITO) or thin, semi-transparent metal films were used for the top electrodes. A 10 nm thick Pt film was typically used for the top electrode, since Pt gave the most reproducible electrical properties; however, thin Au (10 nm), RuO_x (20 nm), and ITO (150 nm) electrodes were also used for comparison.

Hysteresis loops for the films were measured using the Radiant Technologies RT-66A tester. A 200 W Oriel Hg arc lamp in combination with narrow band interference filters was used to generate light at 336, 365, 404, and 436 nm. An argon ion laser was used to produce 457 nm illumination. The illumination intensity was adjusted using neutral density filters. An Ealing optical shutter, which also triggered a voltage supply, was used to control the exposure time. The EPR measurements were made on an X-band Bruker ESP-300E spectrometer at 25K. An optical-access microwave cavity was used for in-situ illumination experiments. Accurate g factors were determined by a frequency counter and an NMR Gaussmeter.

RESULTS

PHOTO-INDUCED EFFECTS

There are two primary phenomena exhibited by PZT and PLZT films that can be used to store optically-generated information. The first type of photo-induced effect common to all PZT and PLZT films studied is illustrated in Fig. 1. The sample for Fig. 1 is an 810 thick $Pb(Zr_{0.53}Ti_{0.47})O_3$ (PZT 53/47) film on $Pt/Ti/SiO_2/Si$. To examine the effect of illumination, the electroded region is initially poled to negative remanence, $-P_r$, where the bottom electrode is at ground with respect to the top electrode. The capacitor is then illuminated with band-gap light (365 nm) through a semi-transparent (12 nm thick) Pt top electrode and biased at +2.5 V, which is near the switching threshold. After a 10 sec exposure with bias, the hysteresis response (solid line) has been altered to exhibit both a clear suppression in the switchable polarization and a noticeable change in the coercive voltage, V_c. The solid curve, which is the new steady-state response, is obtained following several post-illumination hysteresis cycles. This procedure is used because some recovery of the dynamic polarization range, ΔP_s, occurs during the first few

cycles. The change in remanent polarization from the unilluminated to the illuminated response, which is most apparent for this sample at $-P_r$, can be the basis of an optical storage device. The reduction in the value of ΔP_s can be regarded as a photo-induced analog of fatigue. A photo-induced fatigue effect similar to that seen in the thin-film samples is also observed when storing optical images in bulk-ceramic samples of PLZT [9,15].

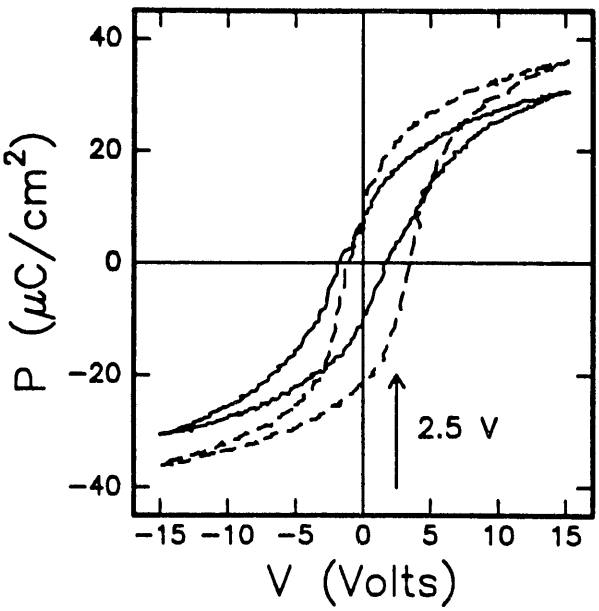

Figure 1. Photo-induced suppression of ΔP by partial switching. PZT 53/47 (810 nm) film on $Pt/Ti/SiO_2/Si$. .... initial response. ____ loop after optical writing. V = +2.5 V, t = 10 sec, λ = 365 nm, I = 25 mW/cm^2.

The compressed loops have been positioned on the polarization axis to reflect a symmetric suppression of the switchable polarization about P=0. A fairly symmetric reduction of ΔP_s has been demonstrated using an electrooptic technique to determine the absolute polarization [15]. The position of the compressed thin-film loops contrasts the behavior observed in PLZT bulk ceramics, where the photo-induced reduction in ΔP is very asymmetric [9,15]. The amount by which ΔP_s and ΔP_r are suppressed is a sensitive function of bias voltage and is maximized by partially switching the material with a bias just below V_c. The initial hysteresis response can be restored by illuminating the sample with a saturating bias of the opposite sign ($-V_s$). Some recovery of ΔP_s (ΔP_r) also occurs due to illumination at $+V_s$, but the restoration is typically incomplete.

The other phenomenon exhibited by all films is a photo-induced shift of the hysteresis loop along the voltage axis, as illustrated in Fig. 2. The sample in this case is a PLZT 6/20/80 (6 at % La) on $Pt/Ti/SiO_2/Si$. The two curves for $+V_s$ and $-V_s$ were obtained after biasing the sample at +15V and -15V, respectively, with concurrent band-gap illumination. This translation of the hysteresis loop implies that a photo-induced, space-charge field has been introduced into the film. The two states produced with the saturating voltages are stable and reproducible end-point states. A pure voltage shift, without optical fatigue, is observed for biases that cause complete switching in contrast to the behavior seen in Fig. 1, which is observed for biases that lead only to partial switching. The magnitude of the maximum shift in coercive voltage, ΔV_c, was measured for a variety of film thicknesses, compositions, electrode materials, and substrate type. It was found that the value of ΔV_c increased with increasing thickness and that for

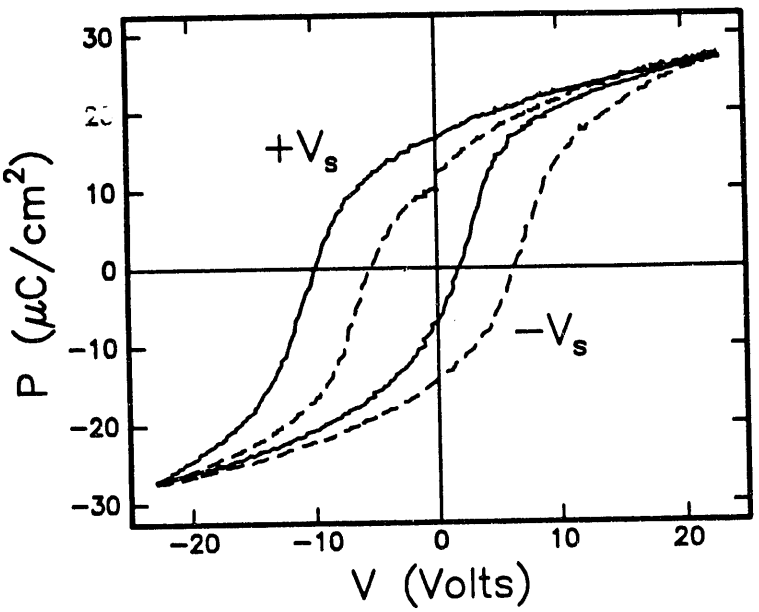

Figure 2. Photo-induced voltage shift indicating the presence of a space-charge field. PLZT 6/20/80 film (1.06 μm) on Pt/Ti/SiO_2/Si.
---- $-V_s$ (-15 V).
—— $+V_s$ (+15 V).
λ = 365 nm, I = 25 mW/cm^2, 20 sec.

a given thickness range, its value did not depend strongly on film composition, electrode material, or substrate type.

Films with relatively square hysteresis loops were used to examine the dependence of the photo-induced voltage shift on the polarization state, as illustrated in Fig. 3. This sample is a 420 nm thick PZT 40/60 film on Pt/MgO. A fairly square hysteresis loop is obtained since the film is both highly oriented and compressively stressed, due to the thermal expansion mismatch with the substrate [16,17]. The loops associated with the two saturating bias states ($+V_s$, $-V_s$) are shown. In addition, Fig. 3 shows the loop obtained after a sample which displayed the $-V_s$ behavior was switched to $+P_r$ and then illuminated at zero bias. The hysteresis loop obtained this way is almost identical to that obtained with a positive saturating bias and light. This result shows that the voltage shift is a direct consequence of the polarization state of the material rather than being a direct function

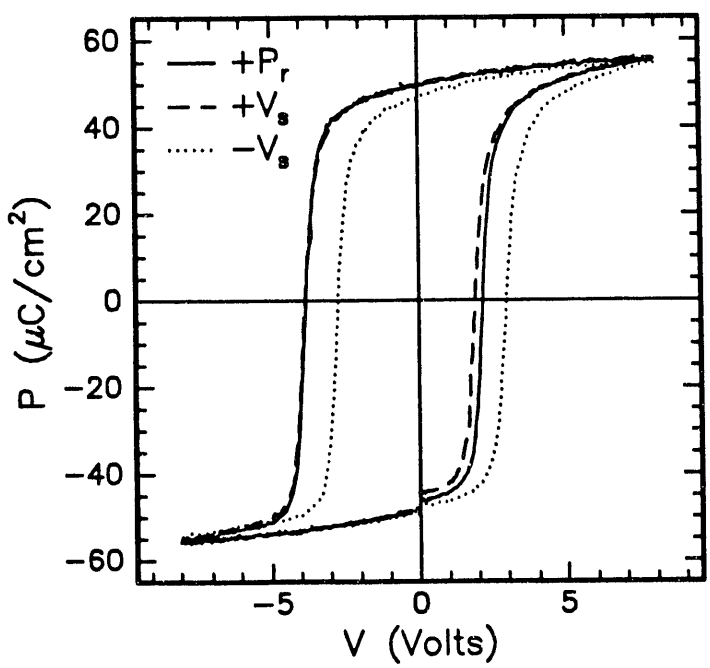

Figure 3. Photo-induced voltage shift for $+P_r$, $+V_s$, $-V_s$. PZT 40/60 film on Pt/MgO (420 nm).
$|V_s|$ = 7V, λ = 365 nm, I = 25 mW/cm^2, t = 20 sec.

of the applied bias. This conclusion is consistent with the observation that the value of ΔV_c does not increase with increasing bias as long as the bias is sufficient to cause complete switching.

KINETIC RESPONSE

Evaluating the time dependence of the photo-induced effects yields mechanistic information and is critical when considering possible device performance. The kinetic response of the voltage-shift effect previously described (Figs. 2 & 3) was determined by measuring the change in coercive voltage obtained when switching from one end-point state to the other as a function of exposure time. Figure 4 illustrates a typical result, which was obtained for a 780 nm thick PZT 40/60 film on oriented Pt/MgO. For each measurement, the sample capacitor was first switched to the negative end-point state using 365 nm light and a bias of -9V applied for 30 sec. Several hysteresis loops were then run to allow for some recovery and to make sure that the initial response was always the same. The 365 nm light and a bias of +9V were then applied concurrently for different periods of time. Finally, several hysteresis loops were run to determine ΔV_c.

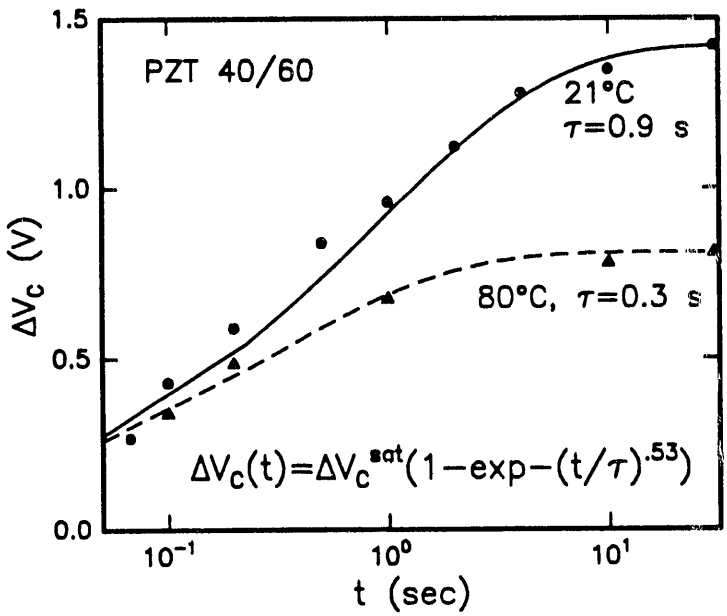

Figure 4. Voltage shift as a function of exposure time for a PZT (40/60) film (780 nm) on Pt/MgO. λ = 365 nm, I=25 mW/cm^2. The lines are fits to the stretched exponential function (Eq. 1).

In general, the voltage-shift kinetics follow a stretched-exponential function of the form,

$$\Delta V_c(t) = \Delta V_c^{sat} [1-\exp-(t/\tau)\beta] \ . \qquad (1)$$

The stretched-exponential dependence is indicative of a dispersive mechanism. Both the stretching parameter, β, and the relaxation time, τ, vary somewhat for different samples; τ is also a function of temperature, illumination wavelength, and light intensity. For the conditions used in Fig. 4 (T = 21°C, λ = 365 nm, and J = 25 mW/cm^2), the stretching parameter had a value of β = 0.53 and a relaxation time of τ = 0.9 sec. The relaxation time decreased to τ = 0.3 sec by increasing the temperature to 80°C. The relaxation time also exhibited a sublinear dependence on the light intensity over the range of 5-25 mW/cm^2. The complete time dependence for the optical-fatigue effect was not characterized; however, a relaxation time of ~ 1 sec is consistent with observations.

SPECTRAL RESPONSE

Another critical aspect of the photosensitivity is the spectral dependence. The spectral dependence of the voltage-shift effect has been evaluated by measuring the value of ΔV_c obtained during a 1 sec exposure with bias using a fixed light intensity. Figure 5 shows a typical result obtained with the 780 nm thick PZT 40/60 film; the writing bias was +9V and the intensity was 25 mW/cm^2. The maximum coercive voltage shift, $\Delta V_c(max)$ = 1.42 V, is obtainable for all five wavelengths given enough time. Therefore, the peak response at 365 nm is equivalent to a minimum in the relaxation time. The main point is that the intrinsic photosensitivity decreases dramatically as a function of energy below the band edge (~3.4 eV).

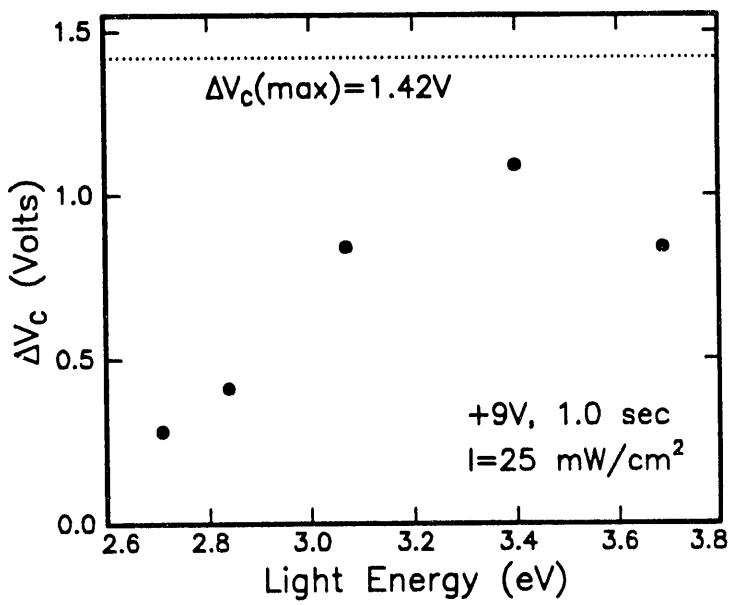

Figure 5. Voltage shift as a function of illumination energy for a 1 sec exposure. I = 25 mW/cm^2, V_s = 9V.

DISCUSSION

The photo-induced changes in hysteresis can be qualitatively accounted for by considering the interaction between internal fields due to the polarization charge and photo-generated carriers. Initially, the situation that occurs due to a saturating bias will be considered. A reasonable domain configuration for an unoriented, columnar film that has been completely switched is schematically depicted in Fig. 6. The arrow head represents the positive terminating end of the spontaneous dipole. The internal charge separation gives rise to a strong depolarizing field. Charge redistribution in the external circuit acts to compensate the polarization charge and, thus, reduce the depolarizing field. However, this charge compensation is typically incomplete. Illuminating the ferroelectric with band-gap light generates electron-hole pairs. The internal depolarizing field acts as a bias to redistribute the photo-generated carriers (+,-), as illustrated. Significant charge redistribution is evidenced by the appearance of a transient photocurrent upon illumination. Trapping of this charge stabilizes the present domain configuration over the oppositely oriented one, which is equivalent to introducing a space-charge field, as shown. This space-charge field leads to the observed voltage shift of the hysteresis loop.

Since the principal polarization discontinuity occurs at the top and bottom electrode interfaces, the internal compensating charge will be trapped near these interfaces. By assuming that essentially all the trapped

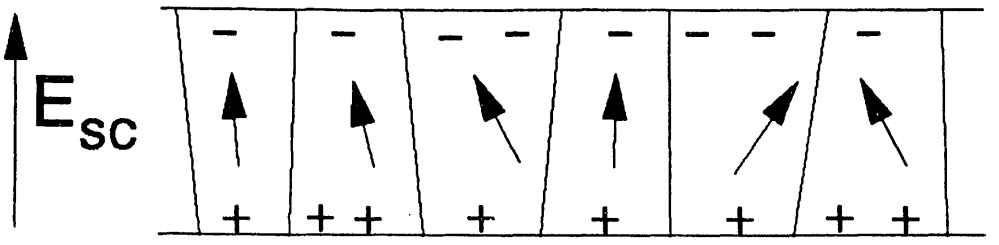

Figure 6. Schematic diagram showing the dipole orientation due to a saturating bias and the internal compensating charge.

charge is at or near the interfaces, ΔV_c is approximately given by,

$$\Delta V_c = \{Q_+(\text{bottom}) + Q_-(\text{top})\} * t/\varepsilon\varepsilon_o \ , \qquad (2)$$

where Q is the charge/unit area and t is the film thickness. For comparable films, the value of ΔVc is expected to increase linearly with thickness, which has been experimentally observed [15]. Equation 2 can then be used to calculate the effective charge/unit area. For the 780 nm thick PZT 40/60 sample on MgO, ΔV_c = 1.42 V and $\varepsilon \simeq 1000$. Assuming $Q_+ \simeq Q_-$, then the effective density of trapped charge near each interface is roughly $5 \times 10^{12}/cm^2$, which is less than 0.1% of the available sites. However, it should also be noted that even though Eq. 2 assumes trapping of both electrons and holes, the phenomenon observed can be sufficiently explained by trapping of primarily one charged species.

The photo-induced fatigue of Fig. 1 can be accounted for by considering the situation that occurs due to partial switching at intermediate biases. Figure 7 depicts a possible domain configuration for a sample with a macroscopic remanent polarization of roughly zero. Photo-generated charge accumulates at domain boundaries with a large polarization discontinuity. This trapped charge inhibits these domains from reorienting. By "locking" the orientation of certain domains, the switchable polarization is reduced.

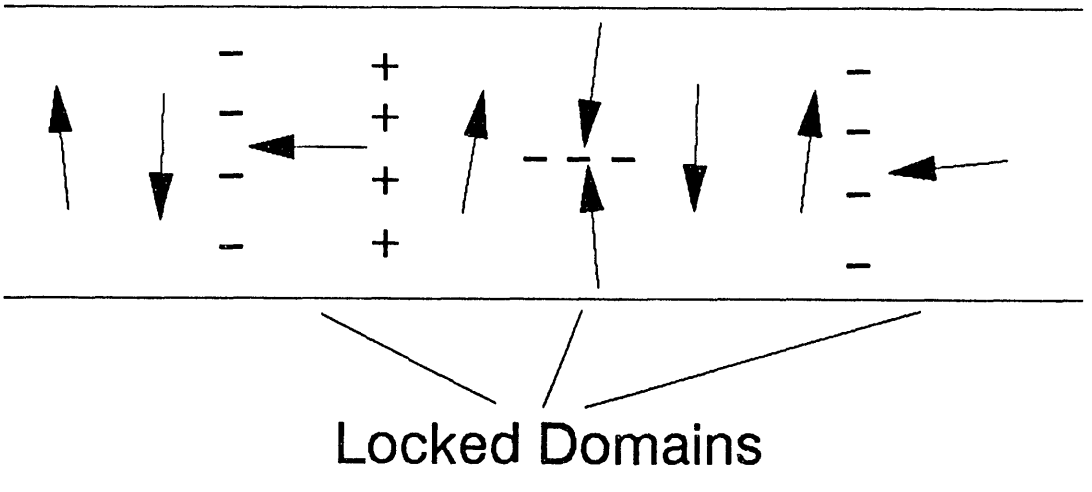

Figure 7. Schematic diagram showing a possible domain configuration for $P \simeq 0$ and the trapped, compensating charge at domain boundaries.

In addition, illumination may allow domain configurations to be established which would ordinarily be unachieveable. For example, the head-to-head domain orientation, which may be possible in thicker films, would normally be energetically unfavorable. However, this configuration would be stabilized by trapped electrons, as shown.

Restoration of the suppressed loop requires near-band-gap illumination to generate new carriers, which can recombine with the trapped charge, and an applied bias to reorient the previously locked domains. An alternative approach would have been to use sub-band-gap illumination to photo-excite the trapped charge out of the trapping centers. Since this approach has not worked, the gap states created by the trapped charge evidently have no optical cross-section. This observation is also consistent with the previously discussed drop in efficiency for the photo-induced effects at wavelengths much below the band edge.

A photo-induced improvement in the initial hysteresis response of films has also been commonly observed. Our most dramatic example of this behavior, which was obtained on the previously described 780 nm thick PZT 40/60 on Pt/MgO, is illustrated in Fig. 8. The initial hysteresis loop of a typical capacitor exhibited low values for P_r and P_s compared to the anticipated response for a highly-oriented, compressed film. Improvement to the light-enhanced loop was achieved with band-gap light and a bias of -8 V for 20 sec. The observation of a photo-induced improvement in hysteresis suggests the presence of processing-induced trapped charge in films. The presence of a large amount of trapped charge in this PZT 40/60 sample was not unreasonable since it was fabricated by rapid thermal annealing using quartz lamps. In addition, this sample, which was annealed twice, displayed a much bigger improvement in the hysteresis than a similar, but thinner sample, which required only one anneal. This difference may be due to the internal interface formed by the initial firing of the thicker film, which could provide an excellent location for charge trapping.

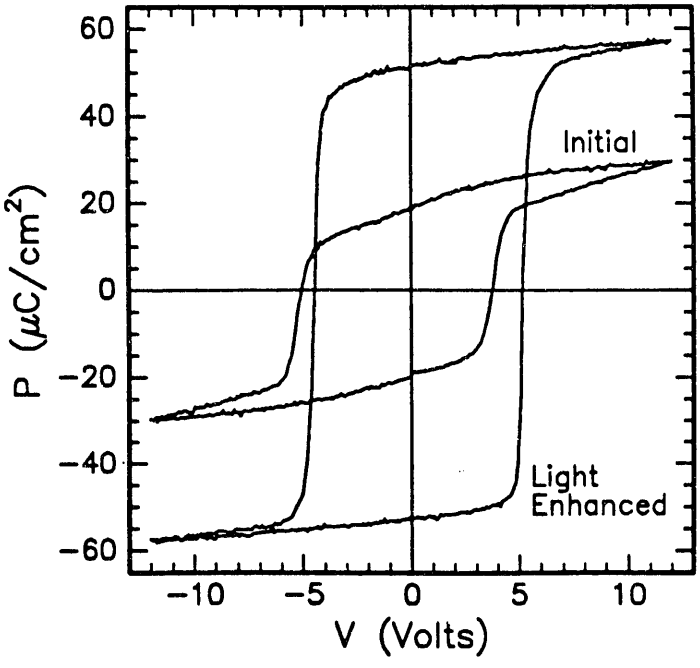

Figure 8. Light-enhanced improvement of the initial hysteresis behvior of a PZT 40/60 film on Pt/MgO. λ = 365 nm, I = 25 mW/cm^2, V = -8 V, 20 sec.

The time response may be controlled by the carrier mobility or the charge-trapping kinetics. If charge migration is rate limiting, the stretched exponential behavior indicates a dispersive transport mechanism. The hole mobility is anticipated to be relatively low due to an abundance of shallow hole traps [18,19]. Alternatively, the trapping kinetics of one or both carrier types into the deeper, more stable traps may be rate limiting for optical storage. In either case, the stretched-exponential kinetics implies a distribution of trapping energies.

The nature of the charge traps have been investigated because of the critical role they play in the photo-induced effects for optical storage. EPR measurements have been done on hot-pressed, ceramic samples of PLZT 7/65/35 [20] and on sol-gel derived powders of various compositions [21]. With band-gap illumination, two-types of charged defects are produced. These defects have been identified as Pb^{+3} and Ti^{+3} [20], as illustrated in Fig. 9b, which is the EPR spectrum for a UV-illuminated PZT 7/65/35 ceramic plate. The Pb^{+3} center is a hole trapped at a Pb^{+2} site; this trapping center is shallow and hence metastable at room temperature [19]. The Ti^{+3} center is an electron trapped at a Ti^{+4} site. Although the Ti^{+3} center is not observed for all samples, the Pb^{+3} center is found for all compositions. It is interesting to note that the creation kinetics of these EPR centers also follows a stretched-exponential function, with a stretching parameter (β) similar to that obtained for the voltage-shift kinetics. This similarity may suggest that both phenomenon are controlled by a common process, such as dispersive carrier transport.

However, there is no obvious relationship between these traps centers and the optical storage effects. Both the Pb+3 and the Ti+3 centers are easily photo-bleached for a range of sub-band-gap wavelengths, as shown in Fig. 7c for a light energy of 2.3 eV. However, photobleaching of these defect centers does not effect the hysteresis loops. Consequently, these

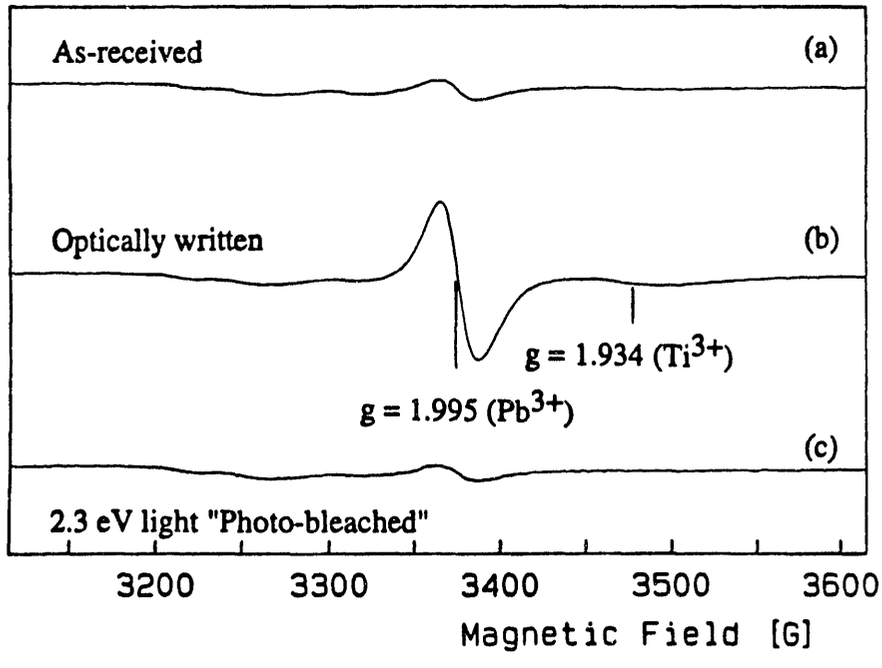

Figure 9. EPR spectra for a PLZT 7/65/35 transparent ceramic sample. The optically written state corresponds to illumination with 365 nm light.

traps can not be the stable ones which control the photo-induced hysteresis changes, which makes sense since they are shallow traps. The lack of any other paramagnetic centers suggest that charges may be trapped as pairs. This situation occurs in systems where the pair trapping is stabilized by a lattice relaxation [22-24]. While it is possible to speculate about the role of various deep defect centers, such as lead vacancies, the critical trapping sites for optical storage effects have not been identified. It is also important to emphasize that the behavior of defects in bulk and powder samples is expected to be the same as for thin films.

CONSIDERATIONS FOR OPTICAL STORAGE DEVICES

The primary requirement for an optical memory or optically-addressable device, such as an SLM, is that light can be used to produce a discernable change in the state of the material. Both types of photo-induced hysteresis changes observed in PLZT films are large and reproducible enough to provide the basis for an optical memory technology. A simple operational scheme for a digital optical memory is illustrated in Fig. 10. Initially the entire sample is reset to the positive curve (+) by switching to $+P_r$ and illuminating. The film is then electrically switched to $-P_r$ with no light. Individual bits are switched to the negative curve (-) by illuminating them one at a time; this procedure allows the bits to be completely defined by the optical addressing process. However, both the illuminated and unilluminated bits are still at $-P_r$. To read the stored information, a bias is applied that partially switches the (+) bits while leaving the (-) bits at $-P_r$. In this case, a pulse of 3.7 V switches the (+) bits to $P_r \approx 0$. This step illustrates the advantage of having a material with a sharp switching threshold. A longer wavelength laser with polarizing optics can be used to differentiate these two states based on the electrooptic response of the material. Since these films exhibit an electrooptic response which is roughly quadratic with respect to polarization ($\Gamma \alpha P^2$) [6], the two

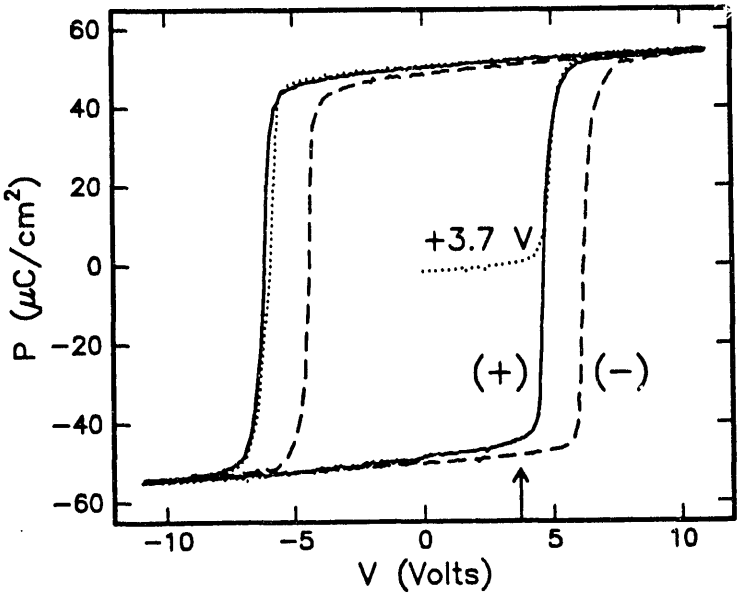

Figure 10. Photo-induced hysteresis response for operation of an optical memory. The arrow corresponds to 3.7 V, which switches the (+) state bits to $P_r \approx 0$.

desireable end-point states are $P_r = |P_r(max)|$ and $P_r = 0$. Selective erasure can be accomplished by electrically switching the film to $+P_r$ and illuminating the bits to be reset, which puts them back on the (+) curve.

While a few different operational mechanisms could be implemented to make a working optical memory using PZT or PLZT films, a number of issues

need to be addressed to produce a competitive technology. To compete with existing hard disk technologies, the time response for writing information needs to be improved by roughly two orders of magnitude. Consequently, it is critical to determine the rate-limiting process and to develop strategies for modifying the response time. An optical-memory medium should also be compatible with solid-state lasers (λ = 700-800 nm). Significant improvements in the photosensitivity at longer wavelenghts can be anticipated based on the improvements achieved in PLZT ceramics by ion implantation [25]. For high-density optical memories, the minimum bit size needs to be evaluated. The bit resolution may depend on both the grain size and the lateral spreading of photo-induced carriers. Finally, the issues common to ferroelectric nonvolatile memories, such as long-term retention, fatigue, and polarization-state imprinting, need to be considered in relation to an optically-addressed, optically-read memory.

CONCLUSIONS

Two different photo-induced changes in hysteresis behavior have been characterized in PZT and PLZT films. The observed effects are controlled by the trapping of charge at the near surface region or at internal domain boundaries. Charge is trapped in very stable centers, which display no paramagnetic signature and, thus, have not yet been identified. A photo-induced improvement in initial hysteresis behavior also demonstrates the presence of processing-induced space charge. The photo-induced voltage shift exhibits a stretched-exponential time dependence, which implies a dispersive mechanism. The relaxation times improve with increasing intensity and increasing temperature, but remain fairly long ($\tau > 0.1$ sec).

Both of the observed photo-induced hysteresis changes could be used to devise a working optical memory; however, there are many issues that need to be resolved to develop a competitive technology. First, the photosensitivity needs to be significantly improved with respect to both the time and spectral dependence. Improvements in the intrinsic photosensitivity of films can be anticipated from chemical doping or ion implantation. Confirming these anticipated improvements will be critical to the development of ferroelectric film optical memories. Second, the minimum bit size needs to be evaluated as compared to the diffraction limit. Third, issues common to ferroelectric memories, such as long-term retention, fatigue, and polarization-state imprinting, need to be considered in relation to an optically-addressed, optically-read memory.

ACKNOWLEDGEMENTS

This work was supported by the Office of Naval Research and the U.S. Department of Energy under contract DE-AC04-76DP00789. The authors would like to acknowledge C.H. Seager, R.W. Schwartz, and J.A. Bullington for helpful discussions and thank D. Goodnow and J. Kubas for technical assistance.

REFERENCES

1. B.A. Tuttle, MRS Bull., 12, [5], 40 (1987).
2. A.R. Tanguay, Opt. Eng., 24, [1], 2 (1985).
3. C.E. Land, Ceram. Trans., 11, 343 (1990).
4. A. Ersen, S. Krishnakumar, V. Ozguz, J. Wang, C. Fan, S. Esener, and S.H. Lee, Appl. Opt., 31, 3950 (1992).
5. S.J. Martin, M.A. Butler, C.E. Land, Elec. Lett., 24, 1486 (1988).
6. D. Dimos, C.E. Land, and R.W. Schwartz, Ceram. Trans., 25, 323 (1992).
7. C.E. Land and P.S. Peercy, Ferroelectrics, 22, 677 (1978).
8. J.W. Burgess, R.J. Hurditch, C.J. Kirkby, and G.E. Scrivener, Appl. Opt., 15, 1550 (1976).
9. P.J. Chen and C.E. Land, J. Appl. Phys., 51, 4961 (1980).
10. C.E. Land, J. Am. Ceram. Soc., 71, 905 (1988).
11. D. Dimos and R.W Schwartz, Mat. Res. Soc. Symp. Proc., 243, 73 (1992).
12. C.E. Land, J. Am. Ceram. Soc., 72, 2059 (1989).
13. R.W. Schwartz, B.C. Bunker, D. Dimos, R.A. Assink, B.A. Tuttle, D.R. Tallant, and I.A. Weinstock, Int. Ferroelectrics, 2, 243 (1992).
14. R.A. Assink and R.W. Schwartz, Chem. of Mater., Accepted for publication (1993).
15. D. Dimos, W.L. Warren, C.H. Seager, B.A. Tuttle, and R.W. Schwartz, submitted to J. Appl. Phys.
16. B.A. Tuttle, J.A. Voigt, T.J. Garino, D.C. Goodnow, R.W. Schwartz, D.L. Lamppa, T.J. Headley,amd M.O. Eatough, Proc. of the 8th IEEE ISAF '92, 344.
17. B.A. Tuttle, J.A. Voigt, and T.J. Headley, accepted for publication J. Am. Ceram. Soc., 76, (1993).
18. V.V. Prisedsky, V.I. Shishkovsky, V.V. Klimov, Ferroelectrics, 17, 465 (1978).
19. J. Robertson, W.L. Warren, D. Dimos, B.A. Tuttle, and D.M. Smyth, submitted to Appl. Phys. Lett.
20. W.L. Warren, C.H. Seager, D. Dimos, and E.J. Friebele, Appl. Phys. Lett., 61, 2530 (1992).
21. W.L. Warren, B.A. Tuttle, P.J. McWhorter, F.C. Rong, and E.H. Poindexter, Appl. Phys. Lett., 62, 482 (1993).
22. W.L. Warren, J. Kanicki, F.C. Rong, E.H. Poindexter,and P.J. McWhorter, Appl. Phys. Lett., 61, 216 (1992).
23. R.A. Street and N.F. Mott, Phys. Rev. Lett. 35, 1293 (1975).
24. P.W. Anderson, Phys. Rev. Lett., 34, 953 (1975).
25. C.E. Land and P.S. Peercy, Ferroelectrics, 45, 25 (1982).

DISCLAIMER

END

DATE
FILMED
9/30/93